Biogeosciences Discuss., 10, 15225–15255, 2013
www.biogeosciences-discuss.net/10/15225/2013/
doi:10.5194/bgd-10-15225-2013

Biogeosciences Discussions
Open Access

Seasonal trends of dry and bulk concentration of nitrogen compounds over a rain forest in Ghana

F. Fattore[1], T. Bertolini[2], S. Materia[2], S. Gualdi[2,4], A. Thongo M'Bou[2], G. Nicolini[2,3], R. Valentini[2,3], A. De Grandcourt[2], D. Tedesco[1], and S. Castaldi[1,2]

[1]DiSTABiF, Seconda Università degli Studi di Napoli, Via A. Vivaldi, 43 – 81100 Caserta, Italia
[2]CMCC, Via A. Imperatore, 16 – 73100, Lecce, Italia
[3]DIBAF, Università della Tuscia, Via San Camillo de Lellis – 01100 Viterbo, Italia
[4]INGV, Via D. Creti, 12 – 40128, Bologna, Italia

Received: 15 August 2013 – Accepted: 30 August 2013 – Published: 17 September 2013

Correspondence to: F. Fattore (ferdinando.fattore@unina2.it)

Published by Copernicus Publications on behalf of the European Geosciences Union.

Abstract

African tropical forests of the equatorial belt might receive significant input of extra nitrogen derived from biomass burning occurring in the north savanna belt and transported equator wards by NE winds. In order to test this hypothesis an experiment was set up in a tropical rain forest in the National park of Ankasa (Ghana) aiming at: quantifying magnitude and seasonal variability of concentrations of N compounds, present as gas and aerosol (dry nitrogen) or in the rainfall (bulk nitrogen), over the studied forest; relating their seasonal variability to trends of local and regional winds and rainfall and to variations of fire events in the region. Three Delta systems, implemented for monthly measurements of NO_2, were mounted over a tower at 45 m height, 20 m above forest canopy to sample gas (NH_3, NO_2, HNO_3, HCl, SO_2) and aerosol (NH_4^+, NO_3^-, and several ions), together with three tanks for bulk rainfall collection (to analyze NH_4^+, NO_3^- and ion concentration). The tower was provided with a sonic anemometer to estimate local wind data. The experiment started in October 2011 and data up to October 2012 are presented. To interpret the observed seasonal trends of measured compounds, local and regional meteo data and regional satellite fire data were analyzed. The concentration of N compounds significantly increased from December to April, during the drier period, peaking in December-February when North Eastern winds (Harmattan) were moving dry air masses over the West central African region and the inter tropical convergence zone (ITCZ) was at its minimum latitude over the equator. This period also coincided with peaks of fire in the whole region. On the contrary, N concentration in gas, aerosol and rain decreased from May to October when prevalent winds arrived from the sea (South-East), during the Monsoon period. Both ionic compositions of rain and analysis of local wind direction showed a significant and continuous presence of see-breeze at site. The ionic composition of rain water resulted much closer to see water and poorer in N compounds from May to October.

BGD
10, 15225–15255, 2013

1 Introduction

Tropical forests have a key role in the terrestrial carbon cycling, acting as the most important global terrestrial C sink and C reservoir. They are the most productive ecosystems on earth, having the higher rate of gross primary productivity (GPP) per surface area and accounting for 34 % of the world's GPP (Beer et al., 2010). The total biomass stock of tropical forests is estimated to be around 247 Gt C, of which 49 %, 25 % and 26 % is attributed to Latin America, sub-Saharan Africa and South-East Asia, respectively (Saatchi et al., 2011). Although old forest stands are generally considered to be a minor sink compared to intermediate stage of forest successions, Lewis et al. (2009) has demonstrated that, in Amazonia, old-growth forests have increased their carbon storage over recent decades and have hypothesized that this might be a pan-tropical phenomenon, probably stimulated by the fertilization effect of increased CO_2 atmospheric concentration. However, several evidences exist that the CO_2 fertilization effect is constrained by N availability and N fertilization (Flischer et al., 2013; Reich et al., 2013). A potential external source for N in forest ecosystems is represented by N depositions (Dise et al., 1995; Gundersen et al., 1998; Rennenberg et al., 1999; Wolff et al., 2010). The source of N deposition can be mainly attributed to combustion of fossil fuels, agricultural practices, animal breeding and fires (Chen et al., 2010; Galloway et al., 1998; Law et al., 2013). The first three sources might account for most of the N depositions observed in industrialized regions and have been hypothesized to stimulate forest growth and C sequestration in Europe (Magnani et al., 2008). In tropical areas, and in particular in Africa, fires might represent the most relevant atmospheric source of extra N for downwind forest ecosystems. Fire-induced losses of N by means of volatilization are substantial (Raison et al., 1985; Cook 1994; Bustamante et al., 2006). Nitric oxide (NO) and ammonia (NH_3) are the primary Nr (reactive N) gases emitted from fires, accounting typically for over 90 % of Nr emissions (Andreae and Merlet, 2001). These gases are converted to other Nr gases (NO_2, HNO_3) and to particulate species (NO_3^-, NH_4^+, and organic aerosols) by means of multiple reaction

BGD
10, 15225–15255, 2013

pathways (Crutzen and Andreae, 1990; Atkinson, 2000). The significant increase of tropical deforestation rates observed in the last century (Houghton and Hackler, 2006) as well as the increased use of land for animal breeding (FAOSTAT database), most often accompanied by the practice of burning in managed pastures, has most probably increased the input of Nr in tropical regions. This phenomenon alone or in combination with increased atmospheric concentration of CO_2 might have stimulated forest growth; however, few data in tropics are available to quantify N depositions so to test this hypothesis, in particular in the African continent.

Based on previous simulations of N deposition by Chen et al. (2010), which supported the concept that a significant amount of N, derived from savanna fires, might be transported equator wards and deposited over tropical forests of the equatorial belt, we set up an experiment in the National park of Ankasa (Ghana), in a rainforest belonging to the west sector of the equatorial African humid forest belt. The work aimed at: 1. quantifying the magnitude and seasonal variability of concentrations of N compounds, which can be detected as gaseous forms and aerosol (dry nitrogen) or can be determined in the rainfall (bulk nitrogen), over the studied forest; 2. relating their seasonal variability to trends of local and regional climatic key variables (winds and rainfalls) which might support the hypothesis of downward atmospheric transport from Northern areas; 3. relating observed variations of dry and bulk nitrogen concentration to variations of fire events in the region.

2 Materials and methods

2.1 Study site

The study was carried out in the Ankasa Wildlife Protected Area (05°16′11.2″N; 02°41′41.55″W) in Ghana, part of a rain forest of about 500 km^2 which became a wildlife protected area in 1976. The site is located about 25 km north of the Guinea coast, slightly north of the equator in West Africa. This location makes the site highly

BGD
10, 15225–15255, 2013

exposed to seasonal shifts of the Inter-Tropical Convergence Zone (ITCZ), that is the area enclosing the globe where the northeast and southeast trade winds converge, allowing strong atmospheric instability and heavy convective precipitation. The movement of air masses in the West Africa is a function of the position of the Inter Tropical Convergence Zone (ITCZ), which separates the hot and dry continental air coming from the Sahara desert (Harmattan) from the cooler, humid maritime air masses (Monsoon) originating from the equatorial Atlantic Ocean (Lebel et al., 2009). In summer, ITCZ moves up to 20° N due to south-western winds associated with the West African Monsoon (WAM, e.g. Thorncroft et al., 2011). This results in several weeks of rainfall in the Sahel region and in the western coasts of North tropical belt. In winter, the maximum convergence is found just south of the Guinea coastline, forced by a predominant northeasterly wind flow that transports hot and dry air from the arid northern regions towards the western coast of central Africa (e.g. Lavaysse et al., 2010). This general synoptic allows a double rain season in Ankasa, with a main peak between April and June and a secondary peak in September-October. On average the mean annual temperature of the site is about 25°C and the mean total annual precipitation is between 1600–2000 mm. The relative humidity is high throughout the year with daily peaks around 90 % at night and 75 % in the early afternoon (Hall and Swaine, 1981).

2.2 Experimental set up

Wind data were collected by a Wind-Master Pro sonic anemometer (Gill Instruments Ltd., UK) placed on the tower at 50 m from soil surface, about 20 m above the canopy layer while precipitation was measured at half-hour resolution by a rain gauge logged with a CR-1000 logger (Campbell Scientific Inc., Logan, UA, USA).

In order to quantify dry (gas and aerosol) concentrations a modified DELTA system (DEnuder for Long-Term Atmospheric sampling, Sutton et al., 2001) was implemented following guidelines of the Co-operative Programme for Monitoring and Evaluation of the Long-range Transmission of Air Pollutants in Europe (EMEP, EMEP/CCC-Report 1/95 Revision 1/2001). The system is based on a set of bore glass denuder

BGD
10, 15225–15255, 2013

traps through which a laminar flow of air is driven by a pump (pumping rates is 0.3–0.4 l min^{-1}) set at the end of the system (Ferm, 1979). A first couple of denuders is coated with citric acid to trap ammonia, a second couple is coated with potassium hydroxide to collect acid gases, HNO_3, SO_2 and HCl. Aerosols pass through the denuders without reacting and then are collected by a couple of filters placed downstream of denuders. These filters are treated with the same alkaline (for the collection of the NH_4^+) and acid (for the collection of NO_3^-, SO_4^{2-}, Cl^-) solutions of denuders (Sutton et al., 2001, Tang et al., 2009). In addition, the system has been set for sampling nitrogen dioxide (NO_2). A method based on absorption of NO_2 on sodium iodide and sodium hydroxide impregnated glass sinter has been developed by Ferm and Sjodin (1993). NO_2 absorbed on the filter is reduced to nitrite (NO_2^-) by iodide (EMEP, EMEP/CCC-Report 1/95 Revision 1/2001). Three DELTA systems were fixed on the tower at 45 m, 20 m above the canopy, each system being protected with a rigid plastic box. Stable sampling rates of 0.38 l min^{-1} are achieved using an air pump with air volumes being measured by a gas meter. Each system contains a sampling train made up of two denuders for ammonia sampling, two denuders for the gaseous acid sampling, one filter for the aerosol ammonium sampling, one filter for the acid aerosols sampling and two glass filters for the sampling of NO_2. Denuders and filters for field sampling were prepared together with laboratory and field/transport blanks. The laboratory blanks were put in labeled grip seal bags and stored in airtight containers in the laboratory where preparation and analyses are carried out (DISTABIF, Italy). A new set of trains and field/transport blanks was sent monthly in polyethylene grip seal bag to the study site and exchanged with the old ones, the field/transport blanks were stored inside the enclosure of the Delta with the new train.

To quantify the bulk concentrations three collectors with funnel of 16 cm diameter were continuously exposed for monthly sampling at the same height of the Delta systems. Biocide (Thymol, 5-methyl-2-[1-methyl]phenol) was added to the collectors to avoid biological alteration of water quality. Every month 100 ml of sample from each

BGD
10, 15225–15255, 2013

collector were filtered (0.45 µm) and transferred into tight plastic bottles for the determination of ion concentrations (EMEP, EMEP/CCC-Report 1/95 Revision 1/2001).

The experiment started on 16 October in 2011, data reported in the paper refer to monthly sampling till 22 October in 2012.

2.3 Laboratory analyses

Bulk samples and exposed trains were shipped to DiSTABiF, being stored at 4 °C until analysis. Acid-coated denuders and aerosols filters were extracted with 3 ml and 4 ml of deionized water, respectively, and analyzed for NH_4^+ using ion chromatography (IC) (Dionex DX-120). Carbonate-coated denuders and filters were extracted with 5 ml of 0.05 % H_2O_2 solution followed by analysis of ions (NO_3^-, SO_4^{2-}, Cl^-) by IC (Tang et al., 2009). The nitrite formed on the glass filter was extracted with deionized water and triethanolamine and its concentration determined by spectrophotometer (Shimadzu UV-1601, SHIMADZU EUROPA GmbH) at 540 nm by the Griess method (EMEP, EMEP/CCC-Report 1/95 Revision 1/2001). Ion Chromatography was used for the determination of the ions (Cl^-, SO_4^{2-}, NO_3^-, Na^+, K^+, Mg^{2+}, Ca^{2+}) in the bulk collection (EMEP, EMEP/CCC-Report 1/95 Revision 1/2001) using a Dionex DX-120, which is a dual column system that performs isocratic ion analyses using conductivity detection. The dual column system allows switching between two sets of ion exchange resin packing columns (guard columns and analytical columns for both anions and cations) and between two eluents. In particular, we have used a Ion Pac AS14A and AG14A guard column for anions, a Ion Pac CS14A analytical column and CG14A guard column for cations, HCO_3/CO_3^{2-} 8 mM buffer and methane sulfonic acid (CH_4O_3S) 0.02 mM to elute anions and cations, respectively. Two self – regenerating suppressors, positioned after the columns, have the function of neutralizing the eluents and enhance analyte conductivity (ASRS ultra 4 mm and CSRS ultra 4 mm for HCO_3^-/CO_3^{2-} and CH_4O_3S, respectively). A detector cell model CDM-3, use a thermistor for temperature compensation.

BGD
10, 15225–15255, 2013

2.4 Data analyses

Dionex Peaknet 6 software was used to compute ionic concentrations from Ion Chromatography analysis. The concentrations of each compounds was multiplied for the extracted volume and divided for the volume measured by the gas meter to obtain the mean concentrations of each sampling. The amount of a trace gas and aerosol collected (Q) on a denuder and filter due to air sampling is given by:

$$Q = (c_e - c_b) \times v \quad (1)$$

where c_e is the liquid concentration of an exposed sample, c_b is the liquid concentration of a blank sample and v is the liquid volume of the extraction solution. The air concentrations (χa) of the trace gas is then determined as:

$$\chi a = Q/V \quad (2)$$

V is the volume of air sampled, which is calculated from the gas meter readings.

Wind data were processed using the EddyPro^{TM} software (LI-COR Inc., Lincoln, NE, USA). In particular, wind vectors were corrected for the angle of attack error (Nakai et al., 2006), rotated (tilt correction) by means of the double rotation method (Wilczak et al., 2001), and screened for the steadiness of horizontal wind (Vickers and Mahrt, 1997).

Meteorological analysis of local and regional data for the period of study was performed using the ERA Interim reanalysis (Berrisford et al., 2009), which provided vertical velocities, meridional and zonal winds. Daily values were filtered through a 30-days running average, in order to filter out the daily noise. Climatic features in the Ankasa location are represented by averaging winds and precipitation over a 1.5°by 1.5°area around the coordinates of the site. Precipitation comes from the Tropical Rainfall Measuring Mission (TRMM, Huffman et al., 2007).

Data of Fire Radiative Power (FRP, in MWatts), which provides information on the measured radiant heat output of detected fires (NASA FIRMS, 2012 http://earthdata.nasa.gov/data/near-real-time-data/firms) were analysed for a region centred

BGD
10, 15225–15255, 2013

in Ankasa, covering an area with a maximum radius of 1000 kilometres, further divided into three concentric areas (0–100, 100–300, 300–1000 km radius). Within each area data for each pixel were first summed to obtain the total MWatts/pixel for each period corresponding to dry and bulk sampling, then the total Mwatts for each area were calculated summing all the pixels falling into each area. These data were used to represent the temporal trend of fires in the area around Ankasa site at different distances for each sampling period.

2.5 Statistical analyses

A One – way analyses of variance (ANOVA) was used to test significant differences among sampling dates for each analyzed compound. When the test was significant an "all pair wise" comparison was carried out based on "Holm – Sidak" method. Tests for normality and equal variance were performed before running parametric tests. To measure the strength of the association between pairs of variables the Pearson Product Moment Correlation was applied.

3 Results

3.1 Annual trends of dry and bulk concentrations

The highest values of NH_3, NO_2 and HNO_3 concentration in the year of sampling were observed from the second half of December 2011 to the second half of April 2012 (Fig. 1). The three gases showed a slightly shift in the peak of concentration, which occurred in December 2011–January 2012 for HNO_3, February 2012–March 2012 for NH_3 and lasted for longer, from Feb 2012 to May 2012, for NO_2. This common trend was also reflected by the correlation analysis which showed a significant correlation of NH_3 with HNO_3 ($P<0.05$, $R = 0.717$) and NO_2 ($P<0.05$, $R = 0.798$).

The NO_3^- concentration in aerosols peaked between December 2011 and January 2012 and was significantly higher in the period between November 2011 to the first half

BGD
10, 15225–15255, 2013

of April 2012, compared with October 2011 and the period between the second half of April 2012 to the end of October 2012 (Fig. 1). The temporal trend of aerosol NO_3^- concentration resembled that of HNO_3, as in fact the two variables were significantly correlated ($P<0.05$, $R = 0.912$). Aerosol NH_4^+ concentration was less variable in time compared with NO_3^-. The amount of N present in the aerosol in form of NO_3^- was generally slightly lower than in form of NH_4^+, except at its peak. NH_4^+ concentration in aerosol was quite constant except a peak in August 2012.

SO_2 concentration was generally quite constant with the exception of the period between mid-November 2011 to Mid-January 2012, when concentration increased significantly almost doubling the values observed during the other months (Table 1). HCl concentration slightly increased between mid-November 2011 to Mid-January 2012 and from half June to half September, while Cl^- concentration in aerosol showed the highest values between April and September 2012 (Table 1). Much more variable was the aerosol concentration of SO_4^{2-} (Table 1).

The mineral nitrogen (NO_3^- and NH_4^+), measured in the bulk depositions, showed a very high variability between and within sampling events (Fig. 2). Similarly to NO_3^- measured in aerosol, bulk NO_3^- concentration peaked between mid-December 2011 and mid-January 2012. As a general trend, the concentration of both ions, NH_4^+ and NO_3^-, in rainfall increased in the period November–January and a decrease afterward (Fig. 2).

The temporal trends of the other bulk compounds (SO_4^{2-}, Cl^-, Na^+, Mg^{2+}, Ca^{2+}) showed higher concentration between June and September 2012 (Table 1), with the exception of K^+, which reached the highest concentration between November 2011 and April 2012 and from June to September. With the exception of Na^+ vs. Ca^{2+} and Cl^- vs. Ca^{2+} the correlation between the different ions measured in rain water was always significant ($P<0.05$), the strongest correlation being the one between Na^+ and Cl^- ($R = 0.991$, $P<0.0001$). The weak correlation between K^+ vs. Na^+, and K^+ vs. Cl^- improved significantly when the data were split into two groups: the first, October 2011–first half of May 2012 ($R = 0,981$ and $R = 0,889$, respectively) and second half of May

BGD
10, 15225–15255, 2013

2012–October 2012 (no significant correlation), which corresponded to sampling during periods characterized by low and high rain regime and different prevailing winds (detailed explanations are given in the next paragraph). The different trend in ionic composition of rain water in these two distinct periods is well described by the triangular plots of Fig. 3. In the first period, characterized by prevailing air masses coming from N-NW, higher NO_3^- and NH_4^+ concentrations in bulk rain water were observed and the ionic composition of rain water was less similar to sea water compared with the second period when air masses were mainly coming from the ocean and the concentration of N in rain was lower.

3.2 Trends of climatic variables and regional fires

Two scales of observation were used to analyze key drivers of transport and deposition, winds and rainfall: a regional (African continent) and a local (Ankasa) one. In Fig. 4 horizontal winds, at 925 hPa and 850 hPa are reported from October 2011 to November 2012. At 925 hPa winds from North-East (Harmattan) prevailed over the whole Western Africa region from December 2011 to January 2012 (Fig. 4). Winds at 850 hPa started to blow from North-East at Ankasa latitude, already in October–November 2011, reaching the equator in December 2011–January 2012 and still persisting over the West African region between February-March 2012. In the same period, in particular between November 2011 and March 2012, rainfall was mostly concentrated on the ocean, in front of West Africa coasts (Fig. 5), over the equator. A slight anomaly was observed in March 2012, when the strength of western monsoon was reduced compared to February and April. For the rest of the analyzed period the rainfall moved northward (Fig. 5) on the continent, driven by the Western African monsoon blowing from the ocean from April to October (Fig. 4). The ITCZ reached its most northerly position in August 2012. Hence the shift of ITCZ leaded to two periods of maximal cloud density at Ankasa latitude, May–July and September–October 2012 (Fig. 5).

Zooming down at Ankasa level, TRMM database was used to quantify local precipitation and vertical wind velocity ($1.5^\circ \times 1.5^\circ$, 30 days averaged value), the latter to

BGD
10, 15225–15255, 2013

evidence periods of convection and subsidence activity. Daily values for this year were filtered through a 30-days running mean, in order to filter out the daily noise. Precipitations (Fig. 6a) showed a bimodal trend. A main and a secondary rainfall peaks occurred in April-July and September-October, respectively, according to the transits of the West African Monsoon over the Guinea Coast and to the vertical wind velocity. The vertical wind velocity at 500 hPa was negative during most of the year, denoting uprising air motion associated with convective activity (Fig 6b). However, from November to March slightly positive (subsidence) values were recorded and from mid-July to end of September values were close to zero.

The amount of rain water sampled on the tower (bulk data) was about 30 % higher than data acquired from TRMM dataset, although a good correlation was found (R = 0.774, P = 0.00865) between the two variables. Wind data from the sonic anemometer located on the top of the Ankasa tower showed that, accordingly with TRMM data, the South West winds prevailed during most of the year, reaching the maximum in July–September (Fig. 7). Northern winds (N, NE and NW) represented only a small percentage of the monthly winds at this observation height and were recorded in October 2011–February 2012 and April–June 2012 (Fig. 7).

The analysis of radiant heat from fires shows that, as expected, maximum values were reached during the drier months (Fig. 8). Fire Radiative Power peaked in December (3.5×10^6 MW) in the area at 300–1000 Km far from Ankasa forest, in February (8×10^4 MW) in the area at 300–100 Km and in March (5×10^3MW) in the area 100–0 Km far from Ankasa (Fig. 8). The three areas differed not only for the peaking month and the strength of the peak but also for the total radiant heat per square meter which was 8.4 MW km^{-2}, 2.6 MW km^{-2} and 1.3 MW km^{-2} for the areas located at 1000–300, 300–100 and 100–0 km from Ankasa, respectively.

BGD
10, 15225–15255, 2013

4 Discussion

The West African climate (and its variability) is a function of the position of the Intertropical Convergence Zone (ITCZ), the frontier between cool and humid marine air mass (monsoon) and warm and dry Saharan air mass (Harmattan) (Lebel et al., 2009). The seasonality of fires and rainfalls in the area is related to these fluctuations. When the ITCZ reaches its most southerly point (<5° N), the whole West African region is characterized by a minimum amount of rainfalls. In fact, in the period between mid November 2011 and mid April 2012, 372 mm of rainwater were measured in the Ankasa site. In the Lamto site (the wet savanna region of Ivory Coast 270 km NW from Ankasa) the mean dry season rainfall reported on average is even lower, 96 mm (Yobouè et al., 2005). In the months from April to mid-November 2012 the ITCZ was moving over continental land of the Western African region northward and back, reaching its maximum latitude in August. Over this whole period, when monsoon winds were strongly prevailing at regional scale, 1610 mm of rainwater were measured at Ankasa. The year 2011–2012 was rather dry in Ankasa, compared with the average of last 10 years (TRMM data). The largest negative anomaly was from March to the end of April 2012, at the beginning of the most intense rain period, when precipitation amounts resulted approximately half the average values reported for the last 10 years (TRMM database). The vertical wind pattern was coherent with this precipitation pattern, including the described anomaly. In fact, vertical wind velocities showed subsidence from December 2011 to March 2012, then fluctuated around the zero till May, when convection should have already triggered (with consequent lower precipitations than expected), reached a maximum of convection in July, coinciding with the peak of precipitation (Fig. 6a, b). Overall, the weak convective activity recorded in year 2012 might be most likely related to the persisting cold anomaly characterizing sea surface temperature (SST) in the Southern tropical Atlantic during most of 2012. Evidence has been provided for the existence of a strong correlation between ocean temperature in this region and rainfall in the coast of Guinea (Joly and Voldoire, 2010).

BGD
10, 15225–15255, 2013

The period, August–September 2012 was characterized by a drastic rainfall drop, which corresponded to the period when the ITCZ was at its most Northerly position (Figs. 4 and 5); in this period vertical wind velocities at Ankasa indicated air subsidence (Fig. 6b).

The shifting between wet periods, during which biomass is produced, and drier periods during which the biomass is turned into highly flammable material, creates conditions for high incidence of fires in the African region which goes from sub-Sahara to equatorial limits. Africa is in fact a fire dominated continent, where about 40 % of all fires of the world occur (Koppman, 2005). The most intense fire period in the Northern African hemisphere typically occurs in November–February (Hao and Liu, 1994; Cooke et al, 1996). In accordance, data for year 2011–2012 showed that fire started in November 2011 and lasted till February 2012 in the savanna belt comprised between 300 and 1000 km from Ankasa. Closer to Ankasa (<300 km) both the fire peak and end of fire season were shifted later in the season. The overall fire intensity decreased going from savannas to rain forest areas (Fig. 8), probably due to more humid conditions found southwards which only allowed for occurrence of fire of moderate strength.

Galanter et al. (2000) have shown that more than 75 % of the atmospheric NO_x found in the northern savanna's belt of Africa is the result of biomass burning that occurs from December to February. Although NO is the main product of biomass burning (Andreae and Merlet, 2001), NO can be quickly transformed to NO_2 and transported at long distances (Crutzen and Andreae, 1990; Atkinson, 2000). At Ankasa, NO_2 concentrations increased from November to April (Fig. 1), corresponding to the whole period of fires occurrence in the Northern African savanna and forest belt (Fig. 8). Two peaks of NO_2 concentrations were recorded, one in February and one in April 2012. The first could be explained by fire peaks recorded at 300–1000 km distance (December) and at 300–100 km (February) which might have produced N compounds, the long range transport of which might have partially overlapped at lower latitudes (close to Ankasa). The second NO_2 peak might instead have coincided with several fire events which were registered near the Ankasa Park in April 2012. The concentration of NO_2 measured at

BGD
10, 15225–15255, 2013

Ankasa during the peak of the fire season (Fig. 1) are comparable to concentrations reported in a rain forest of Southern Cameroon (0.80 $\mu g\,m^{-3}$) and in a northwest Congolese equatorial forest (1.3 $\mu g\,m^{-3}$) during the burning season (Adon et al., 2010). In the period corresponding to the fire season, to lower rainfall and to subsidence of air masses at the Ankasa site, higher values of HNO_3 and NO_3^- in aerosols were recorded as well. HNO_3 is the result of NO_x oxidation and usually is deposited in a wet or dry from within 24 hours from its formation (Huebert and Robert, 1985), while NO_3^- particulate formation can be due to the reaction of HNO_3 with atmospheric base compounds (Seinfeld and Pandis, 1998). This is in accordance with observed values of NO_3^- in aerosols which were significantly correlated with HNO_3 concentrations.

Biomass burning (forest, grassland, and agricultural wastes) is also a significant source of SO_2 to the atmosphere (Bates et al., 1992; Arndt et al., 1997). In fact values of SO_2 concentration at Ankasa site between November and January were twice (up to 0.39 $\mu g\,m^{-3}$) the amount measured in the wetter months (0.17 $\mu g\,m^{-3}$). A comparable increment for both NO_2 and SO_2 atmospheric concentrations was measured by Campos et al. (2010) using passive sampling in a forest area of the Amazon region, at the onset of the dry and fire season.

Equally to the other gaseous compounds also NH_3 concentrations increased significantly between November 2011 and April 2012 at Ankasa (Fig. 1). NH_3 is the primary reactive nitrogen emitted by biomass burning (Andreae and Merlet, 2001). It has a short lifetime in the atmosphere (τ =1–5 days or less) and a relatively high dry deposition velocity, which causes a subsequent substantial fraction (20–40 %) to be deposited not far from its source (Aneja et al., 2001). The statistically significant increase of NH_3 concentration at Ankasa recorded between February and April 2012, coincided with the peak of fire occurrence within an area of 300 km from Ankasa (Fig. 8). Values of NH_3 atmospheric concentrations found in this study are about three to ten times lower than those, measured by Rondon and Sanhueza (1990) with active sampling in a woodland savannah in Venezuela (between the Amazon Forest and the Caribbean Sea) following a biomass burning, while the opposite is true for NO_3^- which was three times higher in

BGD
10, 15225–15255, 2013

the Ankasa site. This difference might be explained also in terms of distance of the fires from the sampling site, as in the Venezuelan study fires were closer to the sampling station, which probably favored higher NH_3 depositions, while NO_3^- in aerosol, which is considered to be a significant component of long-range transported Nr in the atmosphere (Hertel et al., 2006), might have deposited at higher distance from the sampling station.

Taking into account local and regional wind circulation and fire data we can try to explain most of temporal variability of concentration of N compounds, observed at Ankasa. Considering a mean wind velocity of about $4\,m\,s^{-1}$ the air masses from different potential sources located in the area from 300 to 1000 Km far from Ankasa would take about 1 to 3 days to reach the Ankasa tower where, if conditions are favorable, vertical descendant air movements (subsidence) could then deposit at Ankasa the compounds produced during the biomass burning. The winds at 925 hPa which blew from NE in the period November–January might hence have favored the long range transport of HNO_3 and NO_3^- generated from fires in the savanna belt, which peaked around December 2011. As the peak of the fire radiative power came closer to Ankasa also NH_3 concentration started to rise, which corresponded to the period February–April 2012. The 2012 anomaly which created drier conditions in April–May, allowed for a prolonged fire season in the area close to Ankasa (Fig. 8), most probably leading to a second peak of NO_2 in April and high values of NH_3 concentration still observed in April.

The analysis of regional and, most of all, of local winds showed that a significant component of winds coming from S-SE was always present at Ankasa. This effect can be likely attributed to the presence of sea-breezes, long recognized to be an active feature along the Gulf of Guinea coast (Cautenet et al., 1989). The frequency of occurrence of sea breezes shows two regimes characterized by a main peak in the winter and a secondary maximum in May, strongly interacting with the two phases of West African Monsoon regime (Gbambie and Stein, 2012). Sea breezes mainly affect the lower atmosphere layers thus counteracting NE winds at 925 hPa, which prevail only in

BGD
10, 15225–15255, 2013

Dec-Jan at this height. The important role of see-breeze at Ankasa site was confirmed by the analyses of ions in rain water, as in fact, a constant presence of ions with a clear marine origin (Youbouè et al. 2005), such as chloride or sodium, was recorded. The ionic composition of the rainfall (Fig. 3) showed that during the monsoon period, when air masses coming from the ocean brought strong rainfall, the ionic concentration was closer to the composition found in marine water and the amount of nitrogen compounds was minimal whereas the opposite was true during the drier season (Lobert et al., 1990; Delmas et al., 1995; Brocard et al., 1996).

5 Conclusions

Although a direct proof of N origin cannot be provided, this study shows that there is a clear seasonality in the atmospheric concentration of N compounds over this Western Africa rainforest, which is coherent with the dynamics of local and regional meteorological drivers and fire occurrence. The analyses of the whole dataset, supports the idea that fires from the savannah belt might represent a source of N for tropical rain forests located in Southern position, thanks to the regional wind circulation. The next step to understand the potential impact of this phenomenon on forest productivity is to quantify the magnitude of N deposition fluxes over the year.

Acknowledgements. The present work was supported by the ERC grant GHG Africa no. 247349, we thank Justice John Mensah for gas sampling and Paolo Stefani for technical support for the tower. We acknowledge the use of FIRMS data and imagery from the Land Atmosphere Near-real time Capability for EOS (LANCE) system operated by the NASA/GSFC/Earth Science Data and Information System (ESDIS) with funding provided by NASA/HQ.

BGD
10, 15225–15255, 2013

References

Adon, M., Galy-Lacaux, C., Yobouè, V., Delon, C., Lacaux, J. P., Castera, P., Gardrat, E., Pienaar, J., Al Ourabi, H., Laouali, D., Diop, B., Sigha-Nkamdjou, L., Akpo, A., Tathy., J. P., Lavenu, F., and Mougin, E.: Long term measurements of sulfur dioxide, nitrogen dioxide, ammonia, nitric acid and ozone in Africa using passive samplers, Atmos. Chem. Phys., 10, 7467–7487, doi:10.5194/acp-10-7467-2010, 2010.

Andreae, M. and Merlet, P.: Emission of trace gases and aerosols from biomass burning, Global Biogeochem. Cy., 15, 955–966, 2001.

Aneja, V. P., Roelle, P. A., Murray, G. C., Southerland, J., Erisman, J. W., Fowler, D., Asman, W. A. H., and Patni, N.: Atmospheric nitrogen compounds II: emissions, transport, transformation, deposition and assessment, Atmos. Environ., 35, 1903–1911, 2001.

Arndt, R., Carmichael, G. R., Streets, D. G., and Bhatti, N.: Sulfur dioxide emissions and sectorial contributions to sulfur deposition in Asia, Atmos. Environ., 31, 1553–1572, 1997.

Atkinson, R.: Atmospheric chemistry of VOCs and NOx, Atmospheric Environment, 34, 2063–2101, 2000.

Bajamgnigni Gbambie, A. S. and Steyn, D. G.: Sea breezes at Cotonou and their interaction with the West African monsoon, Int. J. Climatol., doi:10.1002/joc.3637, 2012.

Bates, T. S., Lamb, B. K., Guenther, A., Dignon, J., and Stoiber, R. E.: Sulfur emissions to the atmosphere from natural sources, J. Atmos. Chem., 14, 315–317, 1992.

Beer C., Reichstein M., Tomelleri E., Ciais P., Jung M., Carvalhais N., Rödenbeck C., Arain M. A., Baldocchi D., Bonan G. B., Bondeau A., Cescatti A., Lasslop G., Lindroth A., Lomas M., Luyssaert S., Margolis H., Oleson K. W., Roupsard O., Veenendaal E., Viovy N., Williams C., Woodward F. I., and Papale D.: Terrestrial Gross Carbon Dioxide Uptake: Global Distribution and Covariation with Climate, Science 329, 5993, 834–838, 2010.

Berrisford, P., Dee, D. P., Fielding, K., Fuentes, M., Kållberg, P., Kobayashi, S., and Uppala, S. M.: "The ERA-Interim Archive", ERA Report Series, No. 1, ECMWF: Reading, UK, 2009.

Brocard, D., Lacaux C., Lacaux, J. P., Kouadio, G., and Yobouè, V.: Emissions from the combustion of biofuels in western Africa, edited by: J. S. Levine, Global Biomass Burning, MIT Press, Cambridge, 1996.

BGD
10, 15225–15255, 2013

Bustamante, M. M. C., Medina, E., Asner, G. P., Nardoto, G. B., and Garcia-Montiel D. C.: Nitrogen cycling in tropical and temperate savanna, Biogeochemistry, 79, 209–237, doi:10.1007/s10533-006-9006-x, 2006.

Cautenet, S. and Rosset, R.: Numerical simulation of sea breezes with vertical wind shear during dry season at Cape of Three Points, West Africa, Monthly Weather Rev., 117, 329–339, 1989.

Campos, V. P., Cruz L. P. S., Godoi, R. H. M., Godoi, A. F. L., and Tavares, T. M.: Development and validation of passive samplers for atmospheric monitoring of SO_2, O_3 and H_2S in tropical areas, Microchem. J., 96, 132–138, 2010.

Chen, Y., Randerson, J. T., van der Werf, G. R., Morton D. C., Mu, M., and Kasibhatlas, P. S.: Nitrogen deposition in tropical forests from savanna and deforestation fires, Global Change Biol., 16, 2024–2038, doi:10.1111/j.1365-2486.2009.02156.x, 2010.

Cook, G. D.: The fate of nutrients during fires in a tropical savanna, Aust. J. Ecol., 19, 359–365, 1994.

Cooke, W. F., Koffi, B., and Gregoire, J.-M.: Seasonality of vegetation fires in Africa from remote sensing data and application to a global chemistry model, J. Geophys. Res., 101, 21051–21065, 1996.

Crutzen, P. J. and Andreae M. O.: Biomass burning in the tropics – impact on atmospheric chemistry and biogeochemical cycles, Science, 250, 1669–1678, 1990.

Delmas, R., Lacaux, J. P., Menaut, J. C., Abbadie, L., Leroux, X., Helas, G., and Lobert, J.: Nitrogen compound emission from biomass burning in tropical African savanna, FOS/DECAFE Experiment, J. Atmos. Chem., 22, 175–194, 1995.

Dise, N. B. and Wright, R. F.: Nitrogen leaching from European forests in relation to nitrogen deposition, Forest Ecol. Manage., 71, 153–161, 1995.

EMEP Manual for Sampling and Chemical Analysis, EMEP/CCC-Report 1/95, NILU, Kjeller, Norway.

Ferm, M.: Method for determination of atmospheric ammonia, Atmospheric Environment, 13, 1385–1393, 1979.

Ferm, M. and Sjödin, Å.: Proposal of an impregnated filter technique for monitoring of NO_2 at EMEP stations, edited by: Ballman, R., Gehrig, R., Kvalvågnes, I. M., Schaug, J., EMEP Workshop on measurements of nitrogen-containing compounds, Les Diablerets, Switzerland, 173–181, 1992.

BGD
10, 15225–15255, 2013

Flischer, K., Rebel K. T., van der Molen, M. K., Erisman, J. W., Wassen, M. J., van Loon, E. E., Montagnani, L., Gough, G. M., Herbst, M., Janssens, I. A., Gianelle, D., and Dolman, A. J.: The contribution of nitrogen deposition to the photosynthetic capacity of forests, Global Biogeochem. Cy., 27, 187–199, 2013

Galanter, M., Levy II, H., and Carmichael, G. R.: Impacts of biomass burning on tropospheric CO, NO_x, and O_3, J. Geophys. Res., 105, 6633–6653, 2000.

Galloway, J. N.: The global nitrogen cycle: changes and consequences, Environmental Pollution, 102, 15–24, 1998.

Gbambie, A. S. B. and Steyn, D. G.: Sea breezes at Cotonou and their interaction with the West African monsoon, Int. J. Climatol., doi:10.1002/joc.3637, 2012.

Gundersen, P., Emmet, B. A., Kionaas, O. J., Koopmans C. J., and Tietema, A.: Impact of nitrogen deposition on nitrogen cycling in forests: a synthesis of NITREX data, Forest Ecol. Manage., 101, 37–55, 1998

Hall, J. B. and Swaine, M. D.: What is forest, in: Distribution and Ecology of Vascular Plants in a Tropical Rain Forest, Forest Vegetation in Ghana, edited by: Junk, W., The Hague, The Netherlands, 3–29, 1981.

Hao, W. M. and Liu, M.-H.: Spatial and temporal distribution of tropical biomass burning, Global Biogeochem. Cy., 8, 495–503, 1994.

Hertel, O., Skjoth, C. A., Lofstrom, P., Geels, C., Frohn, L. M., Ellermann, T., and Madsen, P. V.: Modelling nitrogen deposition on a local scale – A review of the current state of the art, Environ. Chem., 3, 317–337, 2006.

Houghton, R. A. and Hackler, J. L.: Emissions of carbon from land use change in sub-Saharan Africa, J. Geophys. Res., 111, G02003, doi:10.1029/2005JG000076, 2006.

Huebert, B. J. and Robert, C. H.: The dry deposition of nitric-acid to grass, J. Geophys. Res., 90, 2085–2090, 1985.

Huffman, George J., and Coauthors: The TRMM Multisatellite Precipitation Analysis (TMPA): Quasi-Global, Multiyear, Combined-Sensor Precipitation Estimates at Fine Scales, J. Hydrometeor, 8, 38–55, 2007.

Joly, M. and Voldoire, A.: Role of the Gulf of Guinea in the inter-annual variability of the West African monsoon: what do we learn from CMIP3 coupled simulations?, Int. J. Climatol., 30, 1843–1856, doi:10.1002/joc.2026, 2010.

BGD
10, 15225–15255, 2013

Koppman, R., von Czapiewski, K., and Reid, J. S.: A review of biomass burning emissions, part I: gaseous emissions of carbon monoxide, methane, volatile organic compounds, and nitrogen containing compounds, Atmos. Chem. Phys. Discuss, 5, 10455-10516, 2005.
Lavaysse, C., Flamant, C. and Janicot, S.: Regional-scale convection patterns during strong and weak phases of the Saharan heat low. Atmosph. Sci. Lett., 11, 255–264, doi:10.1002/asl.284, 2010.
Law, B.: Biogeochemistry: Nitrogen deposition and forest carbon, Nature, 496, 307–308, 2013.
Lebel, T. and Ali, A.: Recent trends in the Central and Western Sahel rainfall regime (1990–2007), J.Hydrol., 375, 52–64, 2009.
Lewis, S. L., Lopez-Gonzalez, G., Sonké, B., Affum-Baffoe, K., Baker, T.R., Ojo, L. O., Phillips, O. L., Reitsma, J. M., White, L., Comiskey, J. A., Djuikouo, K. M. N., Ewango, C.E., Feldpausch, T. R., Hamilton, A.C., Gloor, M., Hart, T., Hladik, A., Lloyd. J., Lovett, J. C., Makana, J. R., Malhi, Y., Mbago, F. M., Ndangalasi, H. J., Peacock, J., Peh, K. S., Sheil, D., Sunderland, T., Swaine, M. D., Taplin, J., Taylor, D., Thomas, S. C., Votere, R., and Wöll, H.: Increasing carbon storage in intact African tropical forests, Nature, 457, 1003–1006, doi:10.1038/nature07771, 2009.
Lobert, J. M., Scharffe, D. H., Hao, W. M., and Crutzen, P. J.: Importance of biomass burning in the atmospheric budgets of nitrogen containing gases, Nature, 346, 552–554, 1990.
Magnani, F., Mencuccini, M., Borghetti, M., Berbigier, P., Berninger, F., Delzon, S., Grelle, A., Hari, P., Jarvis, P. G., Kolari, P., Kowalski, A. S., Lankreijer, H., Law, B. E., Lindroth, A., Loustau, D., Manca, G., Moncrieff, J. B., Rayment, M., Tedeschi, V., Valentini, R., and Grace, J.: The human footprint in the carbon cycle of temperate and boreal forests, Nature, 447, 849–851, doi:10.1038/nature05847, 2007.
Nakai, T., van der Molen, M. K., Gash, J. H. C., and Kodama, Y.: Correction of sonic anemometer angle of attack errors, Agricultur. Forest Meteorol., 136, 19–30, 2006.
NASA FIRMS: MODIS Hotspot/Active Fire Detections, Data set, available at: http://earthdata.nasa.gov/firms, 2012.
Raison, R. J., Khanna, P. K., and Woods, P. V.: Mechanisms of element transfer to the atmosphere during vegetation fires, Canad. J. Forest Res., 15, 132–140, 1985.
Reich, P. B. and Hobbie S. E.: Decade-long soil nitrogen constraint on the CO_2 fertilization of plant biomass, Nat. Clim. Change, 278–282, 2013.
Rennenberg, H. and Gessler A.: Consequences of N deposition to forest ecosystems, recent results and future research needs, Water, Air Soil. Pollut., 116, 47–64, 1999.

BGD
10, 15225–15255, 2013

Rondon, A. and Sanhueza, E.: Seasonal variation of gaseous HNO_3 and NH_3 at a tropical savannah site, J. Atmos. Chem., 11, 245–254, 1990.
Saatchi, S. S., Harris, N. L., Brown, S., Lefsky, M., Mitchard, E. T. A., Salas, W., Zutta, B. R., Buermann, W., Lewis S. L., Hagen S., Petrova S., White L., Silman M., and Morel, A.: Benchmark map of forest carbon stocks in tropical regions across three continents, PNAS, 108, 9899–9904, 2011.
Seinfeld, J. H. and Pandis, S. N.: Atmospheric Chemistry and Physics, New York, John Wiley & Sons, Inc., 1998.
Sutton, M. A., Tang, Y. S., Miners, B., and Fowler, D.: A new diffusion denuder system for long-term, regional monitoring of atmospheric ammonia and ammonium, Water, Air Soil Pollut., 1, 145–156, 2001.
Tang, Y. S., Simmons, I., van Dijk, N., Di Marco, C., Nemitz, E., Dammgen, U., Gilke, K., Djuricic, V., Vidic, S., Gliha, Z., Borovecki, D., Mitosinkova, M., Hanssen, J. E., Uggerud, T. H., Sanz, M. J., Sanz, P., Chorda, J. V., Flechard, C. R., Fauvel, Y., Ferm, M., Perrino, C., and Sutton, M. A.: European scale application of atmospheric reactive nitrogen measurements in a low-cost approach to infer dry deposition fluxes, Agricult. Ecosyst. Environ., 133, 183–195, 2009.
Thorncroft, C. D., Nguyen, H., Zhang, C., and Peyrillé, P.: Annual cycle of the West African monsoon: regional circulations and associated water vapour transport, Q. J. R. Meteorol. Soc., 137, 129–147, doi:10.1002/qj.728, 2011.
Vickers, D. and Mahrt, L.: Quality control and flux sampling problems for tower and aircraft data, J. Atmos. Ocean. Technol., 14, 512–526, 1997.
Yobouè, C., Galy-Lacaux, C., Lacaux, J. P., and Siluè, S.: Rainwater chemistry and wet deposition over the Wet Savanna Ecosystem of Lamto (Cote d'Ivoire), J. Atmos. Chem., 52, 117–141, 2005.
Wilczak, J. M., Oncley, S. P., and Stage, S. A.: Sonic anemometer tilt correction algorithms, Bound.-Lay. Meteorol., 99, 127–150, 2001.
Wolff, V., Trebs I., Foken, T., and Meixner, F. X.: Exchange of reactive nitrogen compounds: concentrations and fluxes of total ammonium and total nitrate above a spruce canopy, Biogeosciences, 7, 1729–1744, 2010, http://www.biogeosciences.net/7/1729/2010/.

BGD
10, 15225–15255, 2013

Table 1. Concentration of compounds in dry sampling, gases (bold) and aerosols (italic), and bulk sampling (rainfall). In brackets is reported one standard deviation (n = 3). Each cell value refers to a sampling period which starts at the date indicated in the column heading and ends at the date indicated in the subsequent column.

Dry ($\mu g\,m^{-3}$)											
Date	16/10/11	19/11/11	16/12/12	18/01/12	17/02/12	19/03/12	14/04/12	14/05/12	17/06/12	18/07/12	11/09/12–22/10/12
HCl	0.22 (0.07)	0.37 (0.08)	0.35 (0.04)	0.20 (0.14)	0.17 (0.03)	0.20 (0.09)	0.13 (0.02)	0.25 (0.05)	0.32 (0.03)	0.35 (0.06)	0.18 (0.08)
SO_2	0.21 (0)	0.40 (0.03)	0.30 (0.05)	0.19 (0.03)	0.19 (0.02)	0.19 (0.04)	0.20 (0.03)	0.20 (0.03)	0.22 (0)	0,22 (0)	0.30 (0)
Cl^-	0.91 (0.07)	1.13 (0.30)	1.19 (0.13)	0.87 (0.18)	1.06 (0.13)	1.28 (0.13)	1.34 (0.25)	1.41 (0.17)	2.02 (0.84)	1.33 (0.22)	1.26 (0.18)
SO_4^{2-}	0.48 (0.01)	1.10 (0.27)	1.66 (0.28)	1.39 (0.35)	1.05 (0.02)	0.83 (0.25)	0.68 (0.14)	0.80 (0.25)	2.01 (0.98)	1.45 (0.17)	0.94 (0.05)
Bulk (mg/l)											
Date	16/10/11	19/11/11	16/12/12	18/01/12	17/02/12	19/03/12	14/04/12	14/05/12	17/06/12	18/07/12	7/09/12–12/10/12
Cl^-	2.36 (0.55)	3.63 (0.62)	3.42 (0.51)	4.59 (2.65)	10.94 (6.82)	3.52 (1.95)	1.80 (0.31)	1.70 (0.55)	30.0 (24.0)	18.1 (6.3)	9.13 (4.61)
SO_4^{2-}	0.91 (0.18)	1.60 (0.20)	2.26 (0.23)	1.80 (0.89)	3.92 (2.00)	1.23 (0.55)	0.53 (0.06)	0.52 (0.13)	9.88 (7.34)	4.98 (1.52)	2.17 (0.83)
Na^+	1.60 (0.38)	2.40 (0.52)	2.38 (0.48)	1.90 (0.86)	5.31 (3.26)	2.90 (1.50)	1.51 (0.23)	1.39 (0.33)	20.3 (16.4)	12.6 (5.2)	6.50 (2.54)
K^+	0.31 (0.08)	0.73 (0.39)	0.70 (0.21)	0.52 (0.11)	1.88 (1.03)	1.17 (0.73)	0.26 (0.03)	0.21 (0.07)	1.77 (1.12)	2.39 (2.89)	0.90 (0.59)
Mg^{2+}	0.15 (0.03)	0.25 (0.06)	0.32 (0.04)	0.59 (0.52)	0.84 (0.43)	0.28 (0.08)	0.14 (0.02)	0.12 (0.04)	2.26 (1.78)	1.10 (0.41)	0.52 (0.27)
Ca^{2+}	0.53 (0.07)	0.84 (006)	1.31 (0.11)	1.35 (0.38)	3.56 (1.99)	1.26 (0.39)	0.63 (0.06)	0.42 (0.04)	6.57 (5.39)	1.69 (0.37)	0.69 (0.27)

BGD
10, 15225–15255, 2013

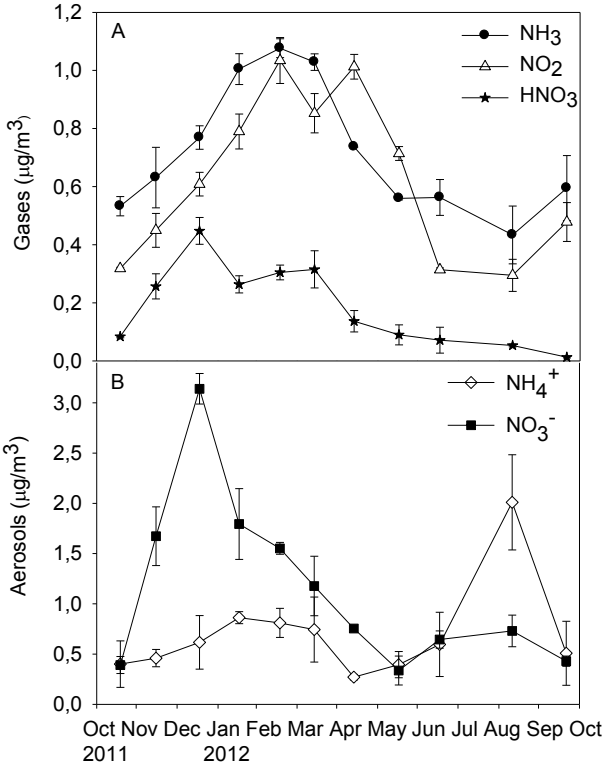

Fig. 1. Temporal trends of **(A)** gaseous (NH_3, NO_2, HNO_3) and **(B)** aerosols (NH_4^+ and NO_3^-) nitrogen compound concentrations measured over the Ankasa tower. Bars represent one standard deviation.

BGD
10, 15225–15255, 2013

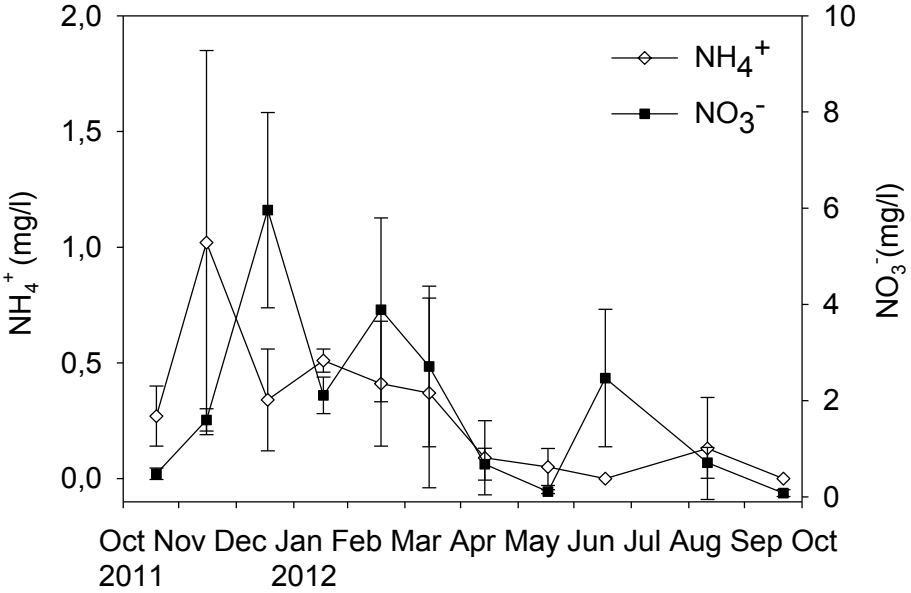

Fig. 2. Temporal trends of NO_3^- and NH_4^+ concentrations in bulk rainfall, measured at Ankasa tower. Bars represent one standard deviation.

BGD
10, 15225–15255, 2013

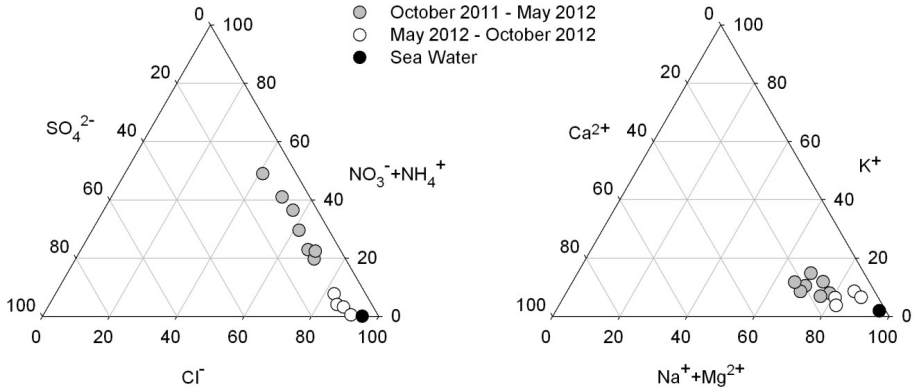

Fig. 3. Triangular diagrams of relative anions **(a)** and cations **(b)** concentrations (mmol l^{-1}) measured in the bulk samplings. Data are divided into two periods corresponding to lower (second half of October 2011 to beginning of May 2012) and higher rain intensity (second half May to beginning of October 2012) and typical ionic values for sea water are also reported.

BGD
10, 15225–15255, 2013

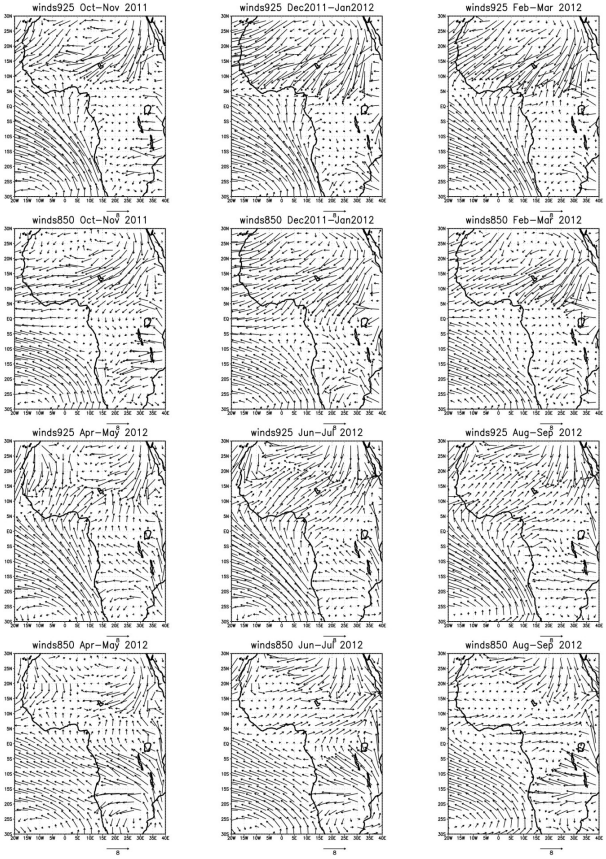

Fig. 4. Bimonthly average wind speed and direction at 925 hPa, 850 hPa ($m\,s^{-1}$) calculated over the African continent from October 2011 to September 2012 from TRMM database.

BGD
10, 15225–15255, 2013

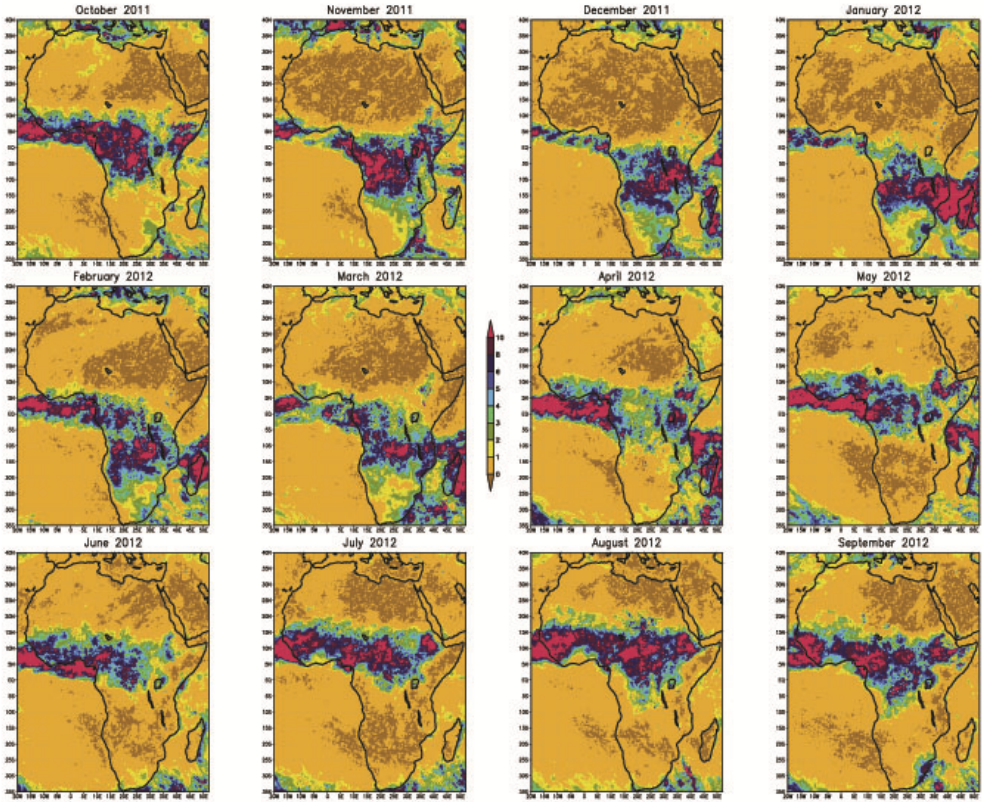

Fig. 5. Total monthly precipitations (mm d^{-1}) calculated over the African continent from October 2011 to September 2012 from TRMM database.

BGD
10, 15225–15255, 2013

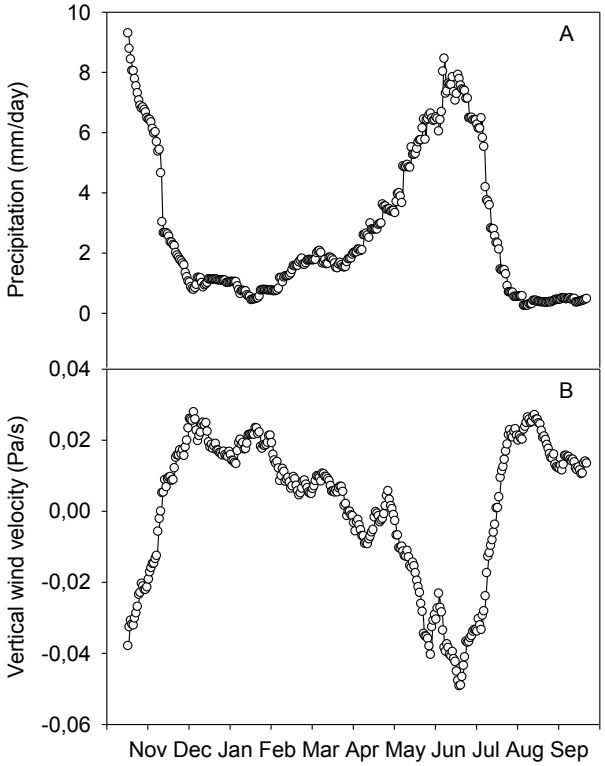

Fig. 6. (A) Total precipitation (mm d^{-1}) and **(B)** vertical velocities at 500 hPa calculated from TRMM database at Ankasa location as 30 days running mean, for the periods between November 2011 and September 2012. Positive values indicate subsidence, negative values denote convection.

BGD
10, 15225–15255, 2013

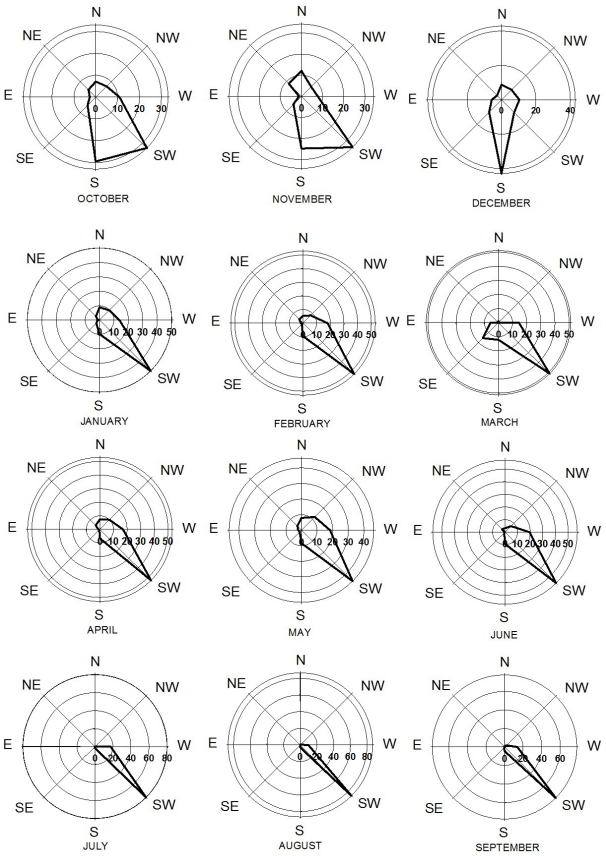

Fig. 7. Polar plots of wind direction data, collected by means of a 3-D sonic anemometer placed at 50 m from the soil (20 m above canopy) on the Ankasa tower. Radius units express the percentage contribution of wind data to eight wind direction sectors (45° degree each).

BGD
10, 15225–15255, 2013

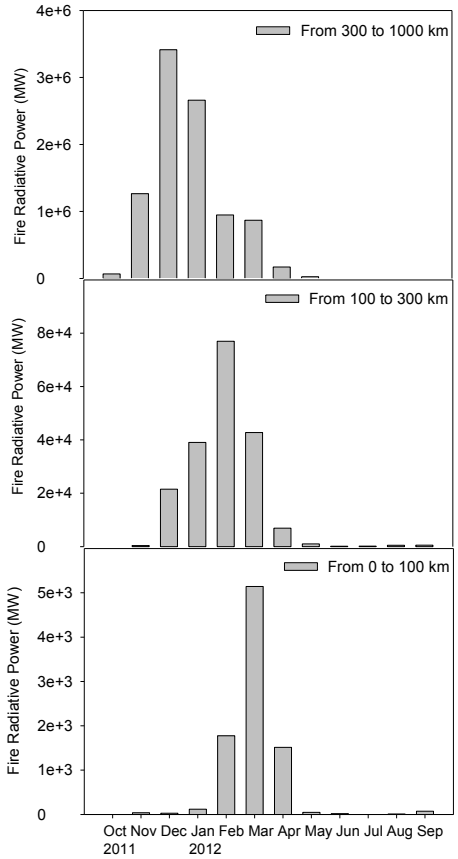

Fig. 8. Monthly total Fire Radiative Power calculated for three concentric areas located at a radial distance of 0–100, 100–300, 300–1000 km from Ankasa, from October 2011 to the end of September 2012.

BGD
10, 15225–15255, 2013